TECHNICAL TRANSACTIONS | **CZASOPISMO TECHNICZNE**
ELECTRICAL ENGINEERING | ELEKTROTECHNIKA
2-E/2015

KRZYSZTOF TOMCZYK, MAREK SIEJA*

PARAMETRIC IDENTIFICATION OF SYSTEM MODEL FOR THE CHARGE OUTPUT ACCELEROMETER

IDENTYFIKACJA PARAMETRYCZNA MODELU SYSTEMU DLA AKCELEROMETRU Z WYJŚCIEM ŁADUNKOWYM

A b s t r a c t

The paper discusses the parametric identification of a system model for the charge output accelerometer based on the simultaneous approximation of amplitude and phase characteristics. The mathematical relationships refer to three models: the mechanical, electrical and complete models, are discussed in detail.

The numerical calculations include the parametric identification of the system model for the PCB357B73 accelerometer and determination of the uncertainties associated with the parameters of this model.

Keywords: *charge output accelerometer*, *parametric identification*

S t r e s z c z e n i e

Artykuł przedstawia parametryczną identyfikację modelu systemu dla akcelerometru z wyjściem ładunkowym opartą na równoczesnej aproksymacji charakterystyk amplitudowej i fazowej. Szczegółowo omówiono w nim matematyczne relacje dotyczące trzech modeli: mechanicznego, elektrycznego i sumarycznego.

Obliczenia numeryczne obejmują parametryczną identyfikację modelu systemu akcelerometru PCB357B73 oraz wyznaczenie niepewności związanych z parametrami tego modelu.

Słowa kluczowe: *akcelerometr z wyjściem ładunkowym*, *identyfikacja parametryczna*

DOI: 10.4467/2353737XCT.15.099.3931

* Ph.D. Eng. Krzysztof Tomczyk, M.Sc. Eng. Marek Sieja, Department of Automatic Control and Information Technology, Faculty of Electrical and Computer Engineering, Cracow University of Technology.

1. Introduction

The identification of the wide range of accelerometers is generally carried out in frequency domain on the basis of the weighted linear least squares method, which allows the easy estimation of the parameters of the mathematical model for the accelerometers in an analytical manner [1, 2]. This mathematical model is, in most cases, presented as the typical system model for the seismic mass accelerometer. The numerator and the denominator of the transfer function of such accelerometers are specified by the constant value and the second degree polynomial respectively. Only if the transfer function contains the constant value in the numerator it is possible to conduct the re-parameterisation procedure of the corresponding complex frequency response – this is performed by dividing the denominator by the numerator of this response and then through the extraction of the two three--component vectors. One of these vectors contains combined parameters, while the second vector consists of the constant values or complex frequency multiplied by the constant values [2–4].

However, in the case of the complete system model for the charge output accelerometer, it is impossible to perform the re-parameterisation procedure because the polynomial occurs in the numerator of the corresponding transfer function. This makes it impossible to apply the analytical weighted least squares method for the parametric identification of this system model. Moreover, it is not possible to determine the resonant frequency and the damping ratio in the same way as for the seismic mass accelerometer, i.e. by means of the first frequency-derivative of the relation referring to the amplitude characteristic.

Both the Monte Carlo (MC) method [5, 6] and the Levenberg–Marquardt (L-M) algorithm [7] are proposed as the identification procedure of the system model for the charge output accelerometer as a response to above mentioned difficulties.

The MC method is used for minimizing the assumed cost function, represented by χ^2 test of matching the complex frequency response of the system model for the charge output accelerometer to the complex frequency response determined on the basis of the measurement data of both frequency characteristics [8–15]. The parameter values of the system model are drawn within the ranges specified by the error margins from the values determined by the L-M algorithm. This algorithm minimizes the objective function, which represents the sum of squared errors between the function describing the amplitude characteristic and the measurement data corresponding to this characteristic.

2. System model for the charge output accelerometer

The complete system model for the charge output accelerometer combines the mechanical and electric models. The system model for the charge output accelerometer can be easily obtained based on the differential equation of the seismic mass accelerometer

$$m\ddot{y}(t) + c\dot{v}(t) + kv(t) = 0 \tag{1}$$

corresponding to the mechanical construction shown in Fig. 1.

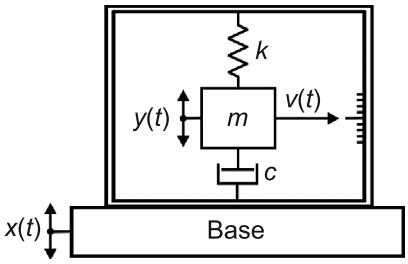

Fig. 1. Mechanical construction of the seismic mass accelerometer

In Figure 1, the following notations are assumed: $v(t)$ – the relative mass displacement (relative output); $y(t)$ – the absolute mass displacement (absolute output); $x(t)$ – the vibration (excitation); m [kg] – the seismic mass; c [kg/s] – the dumping coefficient; k [N/m] – the spring constant; $m\ddot{y}(t)$ – the moment of inertia; $c\dot{v}(t)$ – the moment of dumping; $kv(t)$ – the moment of elasticity.

For the seismic mass accelerometer, the following relation is met:

$$y(t) = v(t) + x(t) \tag{2}$$

and after substitution eq. (2) into eq. (1), we obtain the following differential equation:

$$m\ddot{v}(t) + c\dot{v}(t) + k\dot{v}(t) = -m\ddot{x}(t) \tag{3}$$

which represents the mathematical model of this accelerometer [6, 16].

2.1. Mechanical model for the charge output accelerometer

The response of the charge output accelerometer to the forcing represents the absolute mass displacement $y(t)$. Unlike to the seismic mass accelerometer, it implies the following substitution in eq. (1):

$$v(t) = y(t) - x(t) \tag{4}$$

which gives:

$$m\ddot{y}(t) + c\dot{y}(t) + ky(t) = c\dot{x}(t) + k\,x(t) \tag{5}$$

Transforming eq. (5) to the s – domain, we have:

$$\frac{m}{k}s^2Y(s) + \frac{c}{k}sY(s) + Y(s) = \frac{c}{k}sX(s) + X(s) \tag{6}$$

and

$$\frac{1}{\omega_0^2}s^2Y(s) + \frac{2\beta}{\omega_0}sY(s) + Y(s) = X(s)\left(\frac{2\beta}{\omega_0}s + 1\right) \tag{7}$$

where

$$\omega_0 = \sqrt{\frac{k}{m}}, \quad \beta = \frac{r}{2\sqrt{km}} \tag{8}$$

The quartz crystal deformation by the compression or tension force $F(t)$ generates the electric charge $Q(t)$ on the surfaces of the electrodes connected to the sides of this crystal:

$$Q(t) = k_p F(t) \tag{9}$$

where $k_p = 22 \cdot 10^{-12}$ [C/N] is the piezoelectric constant.

Figure 2 shows the mechanical construction of the charge output accelerometer.

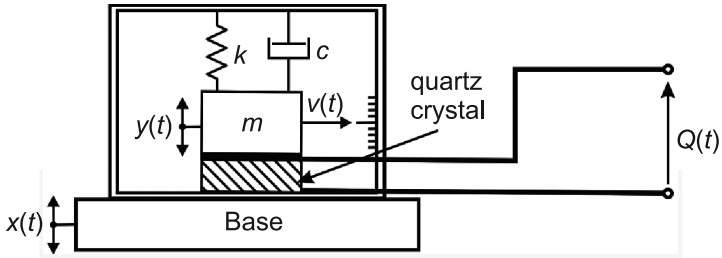

Fig. 2. Construction of the charge output accelerometer

The force that the mass m acts on the crystal is proportional to the absolute acceleration:

$$F(t) = m\ddot{y}(t) \tag{10}$$

Based on eqs. (9) and (10) and after the transformation to the s – domain, we have:

$$Y(s) = \frac{Q(s)}{s^2 m k_p} \tag{11}$$

Substitution eq. (11) into eq. (7) finally yields the mathematical model of the charge output accelerometer:

$$K(s) = \frac{Q(s)}{s^2 X(s)} = S_q \frac{2\beta\omega_0 s + \omega_0^2}{s^2 + 2\beta\omega_0 s + \omega_0^2} \tag{12}$$

where $S_q = k_p S_m$ [C/ms^2] is the charge sensitivity of the accelerometer, while $S_m = m$ [kg] is the mechanical sensitivity of the accelerometer.

2.2. Electrical model for the charge output accelerometer

The conversion of the electric charge $Q(t)$ to the voltage V is carried out by connecting the output of the accelerometer with the voltage amplifier using the low noise coaxial cable. Figure 3 shows the equivalent circuit model for the charge output accelerometer [17].

In Figure 3, the following notations are assumed: Q – the electric charge; R_a, C_a – the internal resistance and capacitance of the accelerometer; R_c – the resistance between cable screen and centre conductor, C_c – the capacitance of the cable, R_i, C_i – the inputs resistance and capacitance of the voltage amplifier.

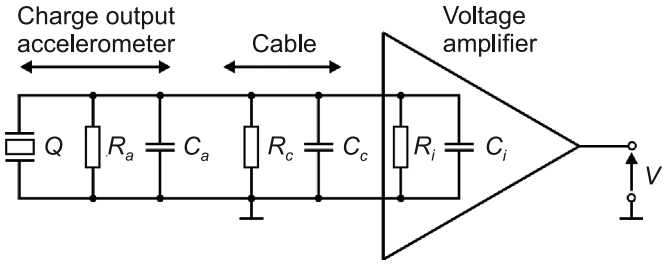

Fig. 3. Equivalent circuit model for the charge output accelerometer

Figure 4 shows the simplified circuit model of the charge output accelerometer, where:

$$R_t = R_a \,//\, R_c \,//\, R_i \tag{13}$$

$$C_t = C_a + C_c + C_i \tag{14}$$

are the total resistance and capacitance.

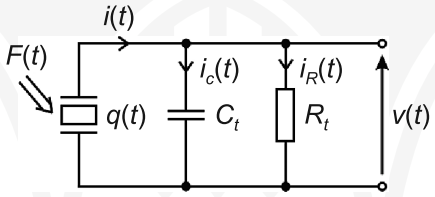

Fig. 4. Simplified circuit model for the charge output accelerometer

Analyzing the circuit shown in Fig. 4, it is easy to get:

$$\frac{V(s)}{Q(s)} = \frac{sR_t}{sR_tC_t + 1} \tag{15}$$

2.3. Complete system model of the charge output accelerometer

Substitution eq. (15) into eq. (12), gives:

$$K(s) = \frac{V(s)}{s^2X(s)} = S_v \frac{s\tau}{s\tau + 1} \frac{2\beta\omega_0 s + \omega_0^2}{s^2 + 2\beta\omega_0 s + \omega_0^2} \tag{16}$$

where $\tau = R_tC_t$ [s] and $S_v = S_eS_m$ [V/ms^2] are respectively the time constant and voltage sensitivity of the complete system model for the charge output accelerometer, and

$$S_e = k_p / C_t \ \text{[V/N]} \tag{17}$$

is the electrical sensitivity.

The frequency characteristics resulting from eq.(16) are as follows:

$$A(\omega) = \\ = S_v\,\tau\,\omega_0\,\omega\sqrt{\frac{\{\omega[\tau\omega_0\omega^2(4\beta^2-1)+\tau\omega_0^3+2\beta\omega^2]\}^2+\{\omega_0\omega^2(2\beta^2-1)+\omega_0^3-2\beta\tau\omega^4\}^2}{[(\omega_0^2-\omega^2-2\beta\tau\omega_0\omega^2)^2++(\tau\omega_0^2\omega-\tau\omega^3+2\beta\omega_0\omega)^2]^2}} \tag{18}$$

and

$$\varphi(\omega) = -\tan^{-1}\frac{\omega_0\omega^2(2\beta^2-1)+\omega_0^3-2\beta\tau\omega^4}{\omega[\tau\omega_0\omega^2(4\beta^2-1)+\tau\omega_0^3+2\beta\omega^2]} \tag{19}$$

3. Identification procedure

Let us present the system model for the charge output accelerometer in the form of the corresponding complex frequency response:

$$K(\omega,\boldsymbol{\theta}) = A(\omega,\boldsymbol{\theta})\exp[j\boldsymbol{\Phi}(\omega,\boldsymbol{\theta})] = S_v\frac{\dfrac{2\beta\omega^2\tau}{\omega_0}-j\omega\tau}{\dfrac{2\beta\omega^2\tau}{\omega_0}+\left(\dfrac{\omega}{\omega_0}\right)^2-1-j\omega\tau\left[1-\left(\dfrac{\omega}{\omega_0}\right)^2+\dfrac{2\beta}{\omega_0\,\tau}\right]} \tag{20}$$

where:

$$\boldsymbol{\theta} = [S_v,\ \omega_{0,},\ \beta,\ \tau] \tag{21}$$

is the vector of the parameters of the complete system model.

It is also assumed that the complex frequency response for the measurement data of amplitude **A** and phase **Φ** is determined as

$$\mathbf{K}(\omega_n) = \mathbf{A}(\omega_n)\exp[j\boldsymbol{\Phi}(\omega_n)], \quad n = 1, 2, \ldots, N \tag{22}$$

The identification procedure is based on eqs. (20)–(22) and includes seven main stages.

In the first stage, on the basis of the vector **A** and by the application of the L-M algorithm, the initial values $\tilde{\boldsymbol{\theta}}_i$ of the vector $\boldsymbol{\theta}$ are determined:

$$\boldsymbol{\theta}_{k+1} = \boldsymbol{\theta}_k^T - [\mathbf{J}^T(\omega,\boldsymbol{\theta}_k)\mathbf{J}(\omega,\boldsymbol{\theta}_k)+\mu_k\mathbf{I}]^{-1}\mathbf{J}^T(\omega,\boldsymbol{\theta}_k)A(\omega,\boldsymbol{\theta}_k), \quad k = 0, 1, \ldots \tag{23}$$

where:

$$\mathbf{J}(\omega,\boldsymbol{\theta}_k) = \begin{bmatrix} \dfrac{\partial A(\omega_0,\boldsymbol{\theta}_k)}{\partial\theta_0} & \dfrac{\partial A(\omega_0,\boldsymbol{\theta}_k)}{\partial\theta_1} & \dfrac{\partial A(\omega_0,\boldsymbol{\theta}_k)}{\partial\theta_2} & \dfrac{\partial A(\omega_0,\boldsymbol{\theta}_k)}{\partial\theta_3} \\ \dfrac{\partial A(\omega_1,\boldsymbol{\theta}_k)}{\partial\theta_0} & \dfrac{\partial A(\omega_1,\boldsymbol{\theta}_k)}{\partial\theta_1} & \dfrac{\partial A(\omega_1,\boldsymbol{\theta}_k)}{\partial\theta_2} & \dfrac{\partial A(\omega_1,\boldsymbol{\theta}_k)}{\partial\theta_3} \\ \vdots & \vdots & \vdots & \vdots \\ \dfrac{\partial A(\omega_{N-1},\boldsymbol{\theta}_k)}{\partial\theta_0} & \dfrac{\partial A(\omega_{N-1},\boldsymbol{\theta}_k)}{\partial\theta_1} & \dfrac{\partial A(\omega_{N-1},\boldsymbol{\theta}_k)}{\partial\theta_2} & \dfrac{\partial A(\omega_{N-1},\boldsymbol{\theta}_k)}{\partial\theta_3} \end{bmatrix} \tag{24}$$

is the Jacobian matrix with $(N-1) \times 4$ dimension and k represents the successive iteration step [6, 7]. In equation (23) $\mathbf{I}$ and μ_k are the 4×4 dimension unit matrix and the variable which changes during each iteration, respectively. The L-M algorithm determines the initial values of the vector parameters for the MC method minimizing the criterion:

$$\tilde{\boldsymbol{\theta}}_i = \min_{\theta} \sum_{n=0}^{N-1} [\mathbf{A}(\omega_n) - A(\omega_n, \boldsymbol{\theta}_k)]^2 \tag{25}$$

In the second stage, the error margins of the vector $\tilde{\boldsymbol{\theta}}_i$ are collated as:

$$\tilde{\boldsymbol{\theta}}_\delta = [\delta_0, \delta_1, \delta_2, \delta_3] \tag{26}$$

In the third stage, the type of the random number generator is selected and the number M of MC trials is assumed.

In the fourth stage, the matrices:

$$\tilde{\mathbf{A}}(\omega, \boldsymbol{\theta}) = \begin{bmatrix} \tilde{A}(\omega_0, \tilde{\boldsymbol{\theta}}_0) & \tilde{A}(\omega_0, \tilde{\boldsymbol{\theta}}_1) & \cdots & \tilde{A}(\omega_0, \tilde{\boldsymbol{\theta}}_m) & \cdots & \tilde{A}(\omega_0, \tilde{\boldsymbol{\theta}}_M) \\ \tilde{A}(\omega_1, \tilde{\boldsymbol{\theta}}_0) & \tilde{A}(\omega_1, \tilde{\boldsymbol{\theta}}_1) & \cdots & \tilde{A}(\omega_1, \tilde{\boldsymbol{\theta}}_m) & \cdots & \tilde{A}(\omega_1, \tilde{\boldsymbol{\theta}}_M) \\ \vdots & \vdots & \ddots & \vdots & \cdots & \vdots \\ \tilde{A}(\omega_n, \tilde{\boldsymbol{\theta}}_0) & \tilde{A}(\omega_n, \tilde{\boldsymbol{\theta}}_1) & \cdots & \tilde{A}(\omega_n, \tilde{\boldsymbol{\theta}}_m) & \cdots & \tilde{A}(\omega_n, \tilde{\boldsymbol{\theta}}_M) \\ \vdots & \vdots & \ddots & \vdots & \cdots & \vdots \\ \tilde{A}(\omega_{N-1}, \tilde{\boldsymbol{\theta}}_0) & \tilde{A}(\omega_{N-1}, \tilde{\boldsymbol{\theta}}_1) & \cdots & \tilde{A}(\omega_{N-1}, \tilde{\boldsymbol{\theta}}_m) & \cdots & \tilde{A}(\omega_{N-1}, \tilde{\boldsymbol{\theta}}_M) \end{bmatrix} \tag{27}$$

and

$$\tilde{\boldsymbol{\Phi}}(\omega, \boldsymbol{\theta}) = \begin{bmatrix} \tilde{\Phi}(\omega_0, \tilde{\boldsymbol{\theta}}_0) & \tilde{\Phi}(\omega_0, \tilde{\boldsymbol{\theta}}_1) & \cdots & \tilde{\Phi}(\omega_0, \tilde{\boldsymbol{\theta}}_m) & \cdots & \tilde{\Phi}(\omega_0, \tilde{\boldsymbol{\theta}}_M) \\ \tilde{\Phi}(\omega_1, \tilde{\boldsymbol{\theta}}_0) & \tilde{\Phi}(\omega_1, \tilde{\boldsymbol{\theta}}_1) & \cdots & \tilde{\Phi}(\omega_1, \tilde{\boldsymbol{\theta}}_m) & \cdots & \tilde{\Phi}(\omega_1, \tilde{\boldsymbol{\theta}}_M) \\ \vdots & \vdots & \ddots & \vdots & \cdots & \vdots \\ \tilde{\Phi}(\omega_n, \tilde{\boldsymbol{\theta}}_0) & \tilde{\Phi}(\omega_n, \tilde{\boldsymbol{\theta}}_1) & \cdots & \tilde{\Phi}(\omega_n, \tilde{\boldsymbol{\theta}}_m) & \cdots & \tilde{\Phi}(\omega_n, \tilde{\boldsymbol{\theta}}_M) \\ \vdots & \vdots & \ddots & \vdots & \cdots & \vdots \\ \tilde{\Phi}(\omega_{N-1}, \tilde{\boldsymbol{\theta}}_0) & \tilde{\Phi}(\omega_{N-1}, \tilde{\boldsymbol{\theta}}_1) & \cdots & \tilde{\Phi}(\omega_{N-1}, \tilde{\boldsymbol{\theta}}_m) & \cdots & \tilde{\Phi}(\omega_{N-1}, \tilde{\boldsymbol{\theta}}_M) \end{bmatrix} \tag{28}$$

are calculated on the basis of the parameters drawn from the ranges

$$\tilde{\boldsymbol{\theta}}_m = [\tilde{S}_{vm} \pm \delta_0, \tilde{\omega}_{0m} \pm \delta_1, \tilde{\beta}_m \pm \delta_2, \tilde{\tau}_m \pm \delta_3] \tag{29}$$

in accordance with the uniform distribution [5, 6].

In the fifth stage, the cost function:

$$\chi^2_m = \sum_{n=0}^{N-1} \frac{\left| \mathbf{K}(\omega_n) - \tilde{K}(\omega, \tilde{\boldsymbol{\theta}}_m) \right|^2}{\sigma^2_{\mathbf{K}(\omega_n)}} \tag{30}$$

for the successive MC trials is calculated, where $\sigma^2_{\mathbf{K}(\omega_n)}$ is the variance of the complex frequency response – eq. (22) [8].

In the sixth stage, both the minimum value of the vector – eq. (30) and corresponding number m_c of MC trials are determined. Resulting from this number, the vector $\tilde{\boldsymbol{\theta}}_c$ is taken as an optimal estimate of the system model for the charge output accelerometer.

In the last stage, the uncertainties associated with the vector $\tilde{\boldsymbol{\theta}}_c$ are determined as the standard deviation of the mean [18]:

$$\hat{\theta}_c^{<r>} = \sqrt{\frac{\sum_{m=0}^{M-1} (\tilde{\theta}_m^{<r>} - \bar{\tilde{\theta}}^{<r>})^2}{M(M-1)}}, \quad r = 0, 1, \ldots, 3 \tag{31}$$

where:

$$\bar{\tilde{\theta}}^{<r>} = \frac{\sum_{m=0}^{M-1} \tilde{\theta}_m^{<r>}}{M} \tag{32}$$

and

$$\tilde{\theta}_m^{<0>} = \tilde{S}_{vm}, \quad \tilde{\theta}_m^{<1>} = \tilde{\omega}_{0m}, \quad \tilde{\theta}_m^{<2>} = \tilde{\beta}_m, \quad \tilde{\theta}_m^{<3>} = \tilde{\tau}_m \tag{33}$$

In order to check the consistency of the measurement data with the system model for the charge output accelerometer corresponding to the vector $\tilde{\boldsymbol{\theta}}_C$, it is proposed to check the criterion:

$$\chi^2_{v,\alpha} \le \sum_{n=0}^{N-1} \frac{\left| \mathbf{K}(\omega_n) - \tilde{K}(\omega, \tilde{\boldsymbol{\theta}}_c) \right|^2}{\sigma^2_{\mathbf{K}(\omega_n)}} \le \chi^2_{v,1-\alpha} \tag{34}$$

where $\chi^2_{v,\alpha}$ is the α – th quantile of the χ^2 distribution of $2N - 4$ degrees of freedom and $\alpha = 0.05$ [2].

4. Results of parametric identification

The procedure discussed in section 3 was applied to the identification of the system model for the PCB357B73 accelerometer with the parameters declared by the manufacturer, i.e. sensitivity S_q = 10.2 pC/ms^2 (±5%), frequency range f_{cut} = 2 kHz (±5%), resonant frequency $f_r \ge 8$ kHz, capacitance C_a = 1500 pF and resistance $R_a = 10^8$ Ω. The PCB cable of the length equals 1 m and the capacitance C_c = 190 pF was used. The measured vectors **A** and **Φ** were determined by the application of the 'back to back' identification procedure [19] supported by LabVIEW software [16], while mathematical calculations were carried out using MathCad14 software [20].

For the L-M algorithm, the input values: $\mu_k = 0.1$ and $\tilde{\boldsymbol{\theta}}_{k=0} = [5.96,\ 57.8 \cdot 10^3,\ 0.1,\ 1.49]$ were assumed. The value of $\tilde{S}_{vk=0}$ was calculated as S_q divided by C_t for C_i = 20 pF, while the value of $\tilde{\tau}_{k=0}$ was determined for R_a = 1 GΩ, R_c = 20 GΩ and R_i = 10 GΩ. The $\tilde{\omega}_{0k=0}$ and $\tilde{\beta}_{k=0}$ were assumed in advance as equal to $57.8 \cdot 10^3$ [rad/s] and 0.1, respectively.

When the objective function for the $k + 1$ iteration step had a value greater than for the step k, the coefficient μ_k was multiplied by the constant value η. The initial value of η was assumed to be equal to 10. In the case of a decrease in the value of the objective function in $k + 1$ iteration step, the coefficient μ_k was divided by η.

For the MC method, two assumptions were made. Firstly, the total number of MC trials were equal to 10^5. Secondly, the percentage deviation of the error margins from the values of the vector $\tilde{\boldsymbol{\theta}}_i$ obtained by means of the L-M algorithm were equal to 5% for each parameter. The determined values of the vector $\tilde{\boldsymbol{\theta}}_i$ were equal to [5.97, $55.90 \cdot 10^3$, 0.21, 1.48].

The frequency, amplitude and phase measurement data for the system model are tabulated in Table 1, where $N = 34$.

Table 1

Frequency, amplitude and phase measurement data

F [kHz]	Amplitude **A** [mV/ms^2]	Phase **Φ** [deg.]	**F** [kHz]	Amplitude **A** [mV/ms^2]	Phase **Φ** [deg.]
0.04	6.1	–0.8	2.0	5.9	–0.2
0.05	6.2	–0.1	2.5	7.0	–0.8
0.06	5.7	–0.1	3.0	6.0	–1.6
0.07	6.0	–0.7	3.5	6.9	–1.2
0.08	6.2	–0.6	4.0	7.6	–2.5
0.09	6.3	–0.4	4.5	8.2	–3.3
0.1	5.7	–0.5	5.0	8.8	–6.1
0.2	5.8	–1.3	5.5	8.8	–9.3
0.3	5.7	–0.2	6.0	10.1	–7.3
0.4	6.1	–0.4	6.5	10.2	–10.2
0.5	5.8	–0.1	7.0	11.2	–19.8
0.6	6.2	–0.1	7.5	13.4	–35.6
0.7	5.7	0	8.0	14.2	–25.9
0.8	6.2	0	8.5	16.5	–37.6
0.9	5.7	–0.6	9.0	14.3	–74.4
1.0	5.9	–0.2	9.5	15.5	–95.6
1.5	6.3	0	10.0	13.8	–97.0

Tables 2 contains the identification results of the system model (second column) with associated uncertainties (fourth column), obtained for $m_c = 86\,540$.

Table 2

Parameters of the vectors $\tilde{\theta}_c$ and $\hat{\theta}_c$

$\tilde{S}_{vc}$ [mV/ms^2]	5.78	$\hat{S}_{vc}$ [mV/ms^2]	$5.46 \cdot 10^{-4}$
$\tilde{\omega}_{0c}$ [rad/s]	$57.37 \cdot 10^3$	$\hat{\omega}_{0c}$ [rad/s]	5.34
$\tilde{\beta}_c$	0.205	$\hat{\beta}_c$	$1.92 \cdot 10^{-5}$
$\tilde{\tau}_c$ [s]	1.56	$\hat{\tau}_c$ [s]	$1.37 \cdot 10^{-4}$

Figure 5 shows the fitting error of system model for the charge output accelerometer.

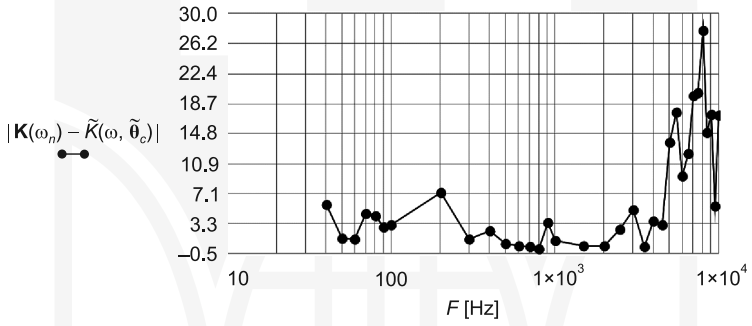

Fig. 5. Fitting error of system model for the charge output accelerometer

Based on Fig. 5, it is easy to notice that the greatest value of fitting error was obtained for the frequency equal to 8 kHz.

For both the measured data and the results of the identification, the criterion – eq. (34) was met, because the value of χ^2 =47.2 was in the range between $\chi^2_{64,0.05} = 46.6$ and $\chi^2_{64,0.95} = 83.7$.

5. Conclusions

The application of both the L-M algorithm only in the first step of the identification procedure, as well as the MC method in the following steps, results most of all from the need to determine the sensitivity from the range of 5% error specified by the manufacturer. The MC method produces the identification results within the ranges providing the practical implementation of the system model. Additionally, the MC method is the procedure recommended by the dedicated standards for determining the uncertainties associated with the parameters of such a system. The L-M algorithm as a gradient procedure works well in the case of the initial calculation of model parameters, which are a basis to the execution

of the MC method. Using only this algorithm for the identification of the system model can lead to results being outside of the non-real ranges for these systems.

Based on the obtained parameters of the system model for the charge output accelerometer, it can be easily noticed that the $\tilde{S}_{vc}$ and $\tilde{\beta}_c$ values are lower while $\tilde{\omega}_{0c}$ and $\tilde{\tau}_c$ values are higher than those obtained by the application of the L-M algorithm. Additionally, the value $\tilde{\beta}_c$ is more than two times higher than that assumed as the input parameter for the L-M algorithm. This means that as an outcome of the MC method execution, the correction of the results obtained based on the L-M algorithm was made by checking the fitting error of the phase characteristic.

References

[1] ISO/IEC Guide 98-3, *Uncertainty of measurement – Part 3: Guide to the expression of uncertainty in measurement*, 2008.

[2] Link A., Täbner A., Wabinski W., Bruns T., Elster C., *Modelling accelerometers for transient signals using calibration measurement upon sinusoidal excitation*, Measurement, 2007, Vol. 40, pp. 928–935.

[3] Tomczyk K., *Modelling of linear analogue transducers in frequency domain*, Przegląd Elektrotechniczny, 2014, No. 6, pp. 202–206.

[4] Tomczyk K., Layer E., *Accelerometer errors in measurements of dynamic signals*, Measurement, 2015, Vol. 60, pp. 292–298.

[5] Kubisa S., *Intuicja i symulacja Monte Carlo podstawą analizy niedokładności pomiarów*, PAK, 2007, No. 9, pp. 3–8.

[6] Layer E., Tomczyk K., *Measurements, modelling and simulation of dynamic systems*, Springer-Verlag, Berlin–Heidelberg–New York 2010.

[7] Tomczyk K., *Levenberg–Marquardt algorithm for optimization of mathematical models according to minimax objective function of measurement systems*, Metrology and Measurement Systems, 2009, Vol. XVI, No. 4, pp. 599–606.

[8] Isermann R., Münchhof M., *Identification of dynamic systems*, Springer-Verlag, Berlin–Heidelberg–Dordrecht–London–New York 2010.

[9] Kollar I., *On frequency-domain identification of linear systems*, IEEE Transactions on Instrumentation and Measurement, 1993, Vol. 42, Issue 1, pp. 2–6.

[10] Pintelon R., Schoukens J., *System identification: A frequency domain approach*, IEEE Press, Piscataway–New York 2001.

[11] Zhao S., Wang F., Xu H., Zhu J., *Multi-frequency identification method in signal processing*, Digital Signal Processing, 2009, Vol. 19, pp. 555–566.

[12] Guillaume P., *Frequency response measurements of multivariable systems using nonlinear averaging techniques*, IEEE Transactions on Instrumentation and Measurement, 1998, Vol. 47, Issue 3, pp. 796–800.

[13] Ljung L., *Some results on identifying linear systems using frequency domain data*, Proc. 32nd IEEE Conf. Decis. Control, San Antonio 1993, pp. 3534–3538.

[14] Sharapov V., *Piezoceramic sensors*, Springer-Verlag, Heidelberg–Dordrecht–London–New York 2011.

[15] Juang J.N., *Applied system identification*, Prentice Hall, Englewood Cliffs 1994.

[16] Tomczyk K., Sieja M., *Acceleration transducers calibration based on maximum dynamic error*, Czasopismo Techniczne, Politechnika Krakowska, No. 3-E/2006, pp. 37–49.

[17] Yu J.Ch., Lan Ch.B., *System modeling and robust design of microaccelerometer using piezoelectric thin film*, Proceedings of the IEEE International Conference on Multisensor Fusion and Integration for Intelligent Systems, Taiwan 1999, pp. 99–104.
[18] BIPM, IEC, IFCC, ILAC, ISO, IUPAC, IUPAP and OIML, Evaluation of measurement data – Supplement 1 to the "Guide to the expression of uncertainty in measurement" – Propagation of distributions using a Monte Carlo method, 2008.
[19] ISO 16063-22, *Methods for the calibration of vibration and shock transducers – Part 22: Shock calibration by comparison to a reference transducer*, 2005.
[20] Tomczyk K., *Special signals in the calibration of systems for measuring dynamic quantities*, Measurement 2014, Vol. 49, pp. 148–152.